Chapter 1

Optical SISO: Exploring the single channel

An optical SISO link can be established between a single transmitting element and a single receiving element. This chapter provides an overview of an optical SISO broadcast channel. It outlines the channel model and provides a mathematical representation of different components involved in the system. An overview of frequently considered optical SISO channel modulation techniques is then provided.

1.1 Coordinate systems

Establishing a coordinate system convention helps to simplify mathematical representation of distances between different devices and signal propagation path lengths. Figure 2·1 illustrates the reference coordinate systems used for all analysis. [$\hat{\mathbf{X}}$ $\hat{\mathbf{Y}}$ $\hat{\mathbf{Z}}$] and [$\hat{\mathbf{x}}$ $\hat{\mathbf{y}}$ $\hat{\mathbf{z}}$] are the basis vectors for the global coordinate system (GCS) and the receiver coordinate system (RCS). A corner of the room in an indoor space is the origin of the GCS while the center of the aperture of the receiver is set as the origin of RCS. The receiver's basis vectors are assumed to always extend parallel to the length, width and surface normal of the sensor.

Let [x_{tx} y_{tx} z_{tx}] be the location of centroid (C_{tx}) of the illumination surface of the transmitter and [x_{rx} y_{rx} z_{rx}] be the location of the centroid of the receiver concentrator

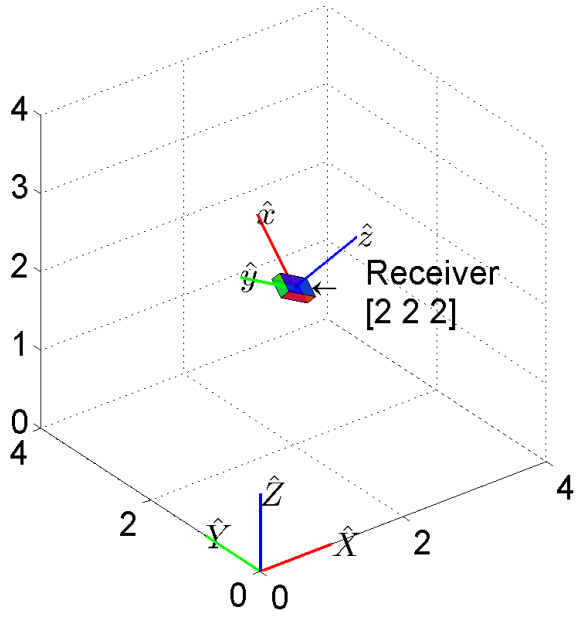

Figure 1·1: Global and receiver coordinate systems

surface in the GCS. The optical axis is then defined by vector $\mathbf{d}$ as calculated in Eq. (2.1) and the vertical distance between the transmitter and receiver is given by $\mathbf{d^z}$ as calculated in Eq. (2.2).

$$\mathbf{d} = \begin{bmatrix} x_{\text{tx}} \\ y_{\text{tx}} \\ z_{\text{tx}} \end{bmatrix} - \begin{bmatrix} x_{\text{rx}} \\ y_{\text{rx}} \\ z_{\text{rx}} \end{bmatrix} \tag{1.1}$$

$$\mathbf{d^z} = (\mathbf{d}.\hat{\mathbf{z}})\hat{\mathbf{z}} \tag{1.2}$$

1.2 Optical SISO channel

A SISO VLC channel can be established between a single luminaire broadcasting information over optical spectrum and a single receiver that can generate an electrical signal proportional to incident optical radiation. Let the radiant flux emitted by the transmitter be represented by x. Intensity modulation imposes a non–negativity constraint ($x \geq 0$) on the transmitted signal. The emitted radiant flux also pro-

vides illumination. Let P_{avg} be the average transmitted radiant flux to maintain user requested illumination levels. Thus mean of transmitted signal must equal P_{avg}.

The transmitted flux propagates through the indoor space and traverses over different paths arriving at the receiver. The received flux can be expressed as a convolution of the channel impulse response and transmitted flux waveform. Under the 'luminaire as a transmitter' model, the LOS component of the received flux is dominant over the NLOS component. In addition to free space path losses, the NLOS component of the received flux undergoes additional attenuation due to non–ideal reflectivity of the walls. The delay spread for the indoor channel is small when compared to frequency of intensity modulation. Under these circumstances, the channel can be treated as a LOS channel and the channel impulse response can be represented by a single tap with gain h.

At the receiver, additive noise independent of the signal is added to the received signal and represented by w. Let the total received signal and noise be represented by y. The system can then be represented as in Eq. (2.3).

$$y = hx + w \tag{1.3}$$

The channel gain is a function of the radiant intensity of flux emission, the free space square path loss, optical gains at receiver and receiver sensor responsivity. Let the radiant intensity emitted by the transmitter at any angle ϕ subtended between the transmitter surface normal and the optical axis be given by $L(\phi)$. Radiant intensity of a Lambertian transmitter of order m is given by

$$L(\phi) = \begin{cases} \frac{(m+1)}{2\pi} cos^m(\phi) & ; -\pi/2 \leq \phi \leq \pi/2 \\ 0 & ; \text{ else} \end{cases} \tag{1.4}$$

The SISO receiver optics comprises of an optical concentrator. Incorporating a

concentrator helps increase the effective area of the sensor. This enables the receiver to incorporate a sensor with smaller dimensions thus reducing its capacitance and enabling a higher receiver bandwidth. Additionally sensor with smaller dimensions enables a compact form factor which can then enable its integration within portable devices. Let ψ be the angle between the receiver surface normal ($\hat{\mathbf{z}}$) and the optical axis ($\mathbf{d}$). Let η be the refractive index of the material of the concentrator and ψ_c be the field of view of the concentrator. Then the optical concentrator gain is given by

$$G(\psi) = \begin{cases} \frac{\eta^2}{sin^2(\psi_c)} & ; 0 \leq \psi \leq \psi_c \leq \frac{\pi}{2} \\ 0 & ; \psi > \psi_c \end{cases} \tag{1.5}$$

Let $S(\lambda)$ be the normalized SPD of the normalized emitted radiant flux such that area under curve is 1 W. Let $R(\lambda)$ be the responsivity of the PD. An optical filter can be incorporated within the receiver to provide selectivity to wavelengths of interest and reject unwanted optical radiation thus reducing noise. Depending on construction of optical filter, its transmittance is a function of angle of incidence and wavelength of radiation. Let the transmittance of the filter be given by $T(\psi, \lambda)$. Thus the effective responsivity of the receiver including the transmission and gains from all optical components is given by

$$R_e(\psi) = G(\psi) \int_{\lambda_{min}}^{\lambda_{max}} S(\lambda) T(\psi, \lambda) R(\lambda) d\lambda \tag{1.6}$$

where λ_{min} to λ_{max} span all the wavelengths of interest.

Let A be the active area of the PD. The overall channel gain h is a function of the parameters discussed above and is then given by

$$h = L(\phi) \frac{A}{||\mathbf{d}||^2} cos(\psi) R_e(\psi) \tag{1.7}$$

Average flux incident on a PD introduces shot noise within the optical-to-electrical conversion process. In a typical SISO VLC link, shot noise from ambient illumination dominates over that from signal (Barry, 1994). Let q be the charge of an electron. Worst cast shot noise from isotropic ambient radiant flux $P_a(\lambda)$ is then given by

$$\sigma_{sh}^2 = \frac{2qAG(\psi_c)}{\psi_c} \int_{\lambda_{min}}^{\lambda_{max}} \int_{0}^{\psi_c} P_a(\lambda) R(\lambda) T(\psi, \lambda) d\psi d\lambda \tag{1.8}$$

Statistics of shot noise are typically Poisson in nature. For a large mean, a Poisson random variable can be approximated by a normal distribution with same variance. Thus, for the optical channel, shot noise is assumed to be distributed normally with variance σ_{sh}^2.

The TIA is generally the first current to voltage amplifier stage after the PD. In the absence of significant ambient illumination, the TIA noise is the dominant source of noise (Kahn and Barry, 1997). The thermal noise from the TIA is considered as the dominant electronic noise component and is given by (Kahn and Barry, 1997),

$$\sigma_{th}^2 = \frac{4kT}{R_f} \tag{1.9}$$

where k is the Boltzmann's constant, T is the absolute temperature and R_f is the feedback resistance of the TIA.

Thus the total noise current density can be computed from the shot noise current density and thermal noise current density. It is additive, white and Gaussian its variance is given by

$$\sigma_n^2 = \sigma_{sh}^2 + \sigma_{th}^2 \tag{1.10}$$

While P_{avg} is the average transmitted radiant flux and let B be the signal bandwidth. Using the parameters described above the SISO channel's SNR can be defined

by Eq. (2.11).

$$\text{SNR} \triangleq \frac{(hP_{avg})^2}{\sigma_n^2 B} \tag{1.11}$$

1.3 Modulation techniques

The optical carriers span the electromagnetic spectrum within 380 THz – 780 THz range. Lack of adequate electronics for passband transmission or reception at such high frequency ranges makes it impractical to implement coherent signaling schemes. However, it is possible to vary the intensity of such spectrum at the transmitter and detect it directly by optical flux to electrical signal conversion at the receiver. Thus, modulation techniques are implemented in conjunction with IM/DD to transfer information using the optical spectrum. A number of different modulation techniques have been studied for RF wireless communications. Some of those have been adapted for OWC due to the unique constraints of the optical channel. This section provides a summary of the more popular SISO modulation techniques.

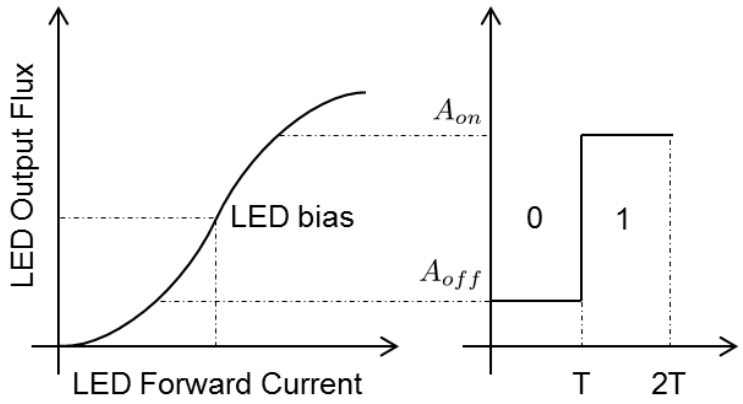

Figure 1·2: Optical OOK signals

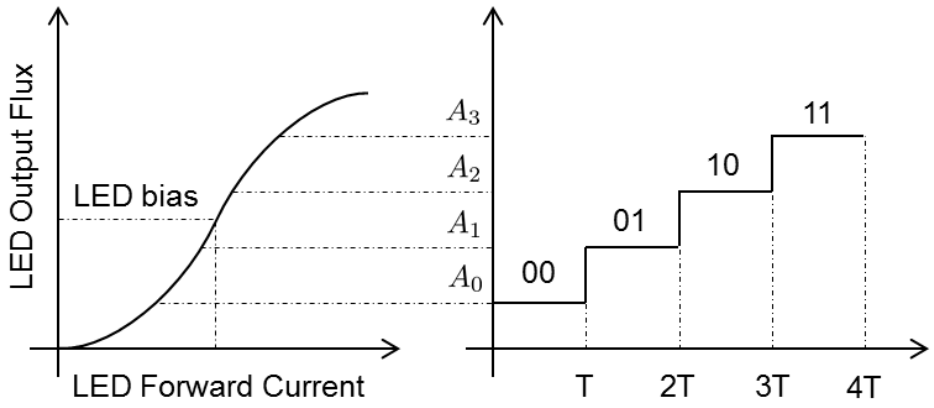

Figure 1·3: Optical 4-PAM signals

1.3.1 On-off keying

As the name suggests, OOK transmits information in the form of presence (on) or absence (off) of light. It is typically implemented under the NRZ model. To transmit bit '0', the transmitter drives all LEDs at a low intensity level and to transmit bit '1', it drives them all to a high intensity level. The on and off intensity levels can be set to achieve a desired average illumination level. Figure 2·2 illustrates the OOK signal waveforms. A_{off} is the low intensity radiant flux and A_{on} is the high intensity radiant flux emitted by the LEDs at the off and on levels. If p is the probability of transmitting bit '1', the average transmitted flux given by $A_{avg} = (1-p)A_{off} + pA_{on}$ is used to provide illumination whereas flux $A_{com} = p(A_{on} - A_{off})$ is used for communication. OOK-NRZ has a spectral efficiency of 2 bits/Hz. References (Komine and Nakagawa, 2004; Vucic et al., 2009) have demonstrated feasibility of OWC in indoor spaces while providing illumination using OOK.

1.3.2 Pulse amplitude modulation

M-ary PAM can transfer information by varying the amplitude of each transmitted pulse. m=$\log_2(M)$ bits to transmit are mapped to one out of M possible pulse

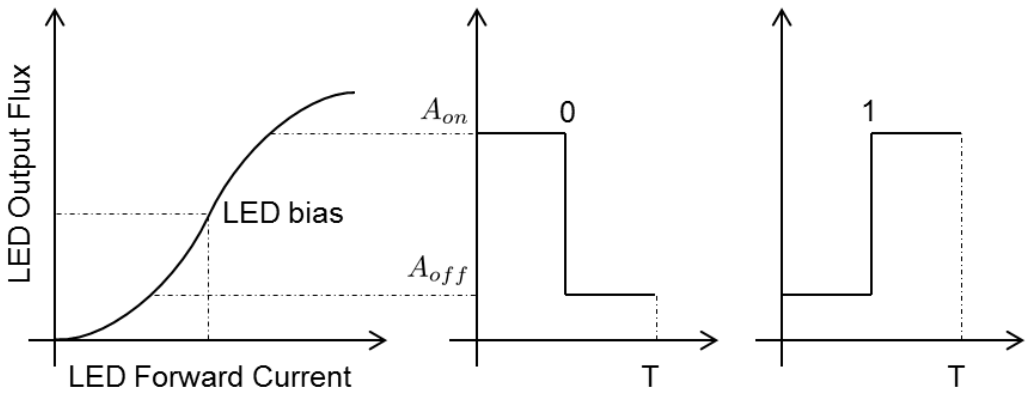

Figure 1·4: Optical 2-PPM signals with 50% duty cycle.

amplitudes. To transmit m bits, the transmitter then drives all LEDs to emit radiant flux corresponding to the mapped amplitude. Let A_{lo} be the lowest pulse amplitude and A_{hi} be the highest pulse amplitude, then the M different amplitude levels are given by $A_i = A_{lo} + i \times (A_{hi} - A_{lo})(M-1); 0 \leq i < M$. For equi-probable bits, flux given by $A_{avg} = (A_{lo} + A_{hi})/2$ is used to provide illumination whereas flux $A_{com} = (A_{hi} - A_{lo})/2$ is used for communication. Figure 2·3 illustrates the 4-PAM signal waveforms. References (Grubor et al., 2008) have demonstrated M-ary PAM for OWC in indoor spaces while providing illumination.

1.3.3 Pulse position modulation

M-ary PPM can transfer information by varying the temporal offset (position) for the low-high edge of each transmitted pulse. The amplitude and duty cycle of each pulse is kept constant. m=$\log_2(M)$ bits to transmit are mapped to one out of M possible pulse offsets. To transmit m bits, the transmitter drives all LEDs to emit a constant flux for a constant pulse on-time starting at a corresponding mapped temporal offset. Let A_{off} be the low intensity radiant flux emitted during the off time of each pulse period and A_{on} be the high intensity radiant flux emitted by the LEDs during the on time of each pulse period and let d be the pulse duty cycle. Then irrespective of the

distribution on the information bits, flux given by $A_{avg} = (1-d)A_{off} + dA_{on}$ is used to provide illumination whereas flux $A_{com} = d(A_{on} - A_{off})$ is used for communication. Figure 2·4 illustrates 2-PPM signal waveforms. References (Bai et al., 2010) have demonstrated using PPM for illumination and communication. VPPM, a variation on PPM, has been proposed in IEEE 802.15.7 as a means to achieve dimming along with data communications. In M-ary VPPM, the information to transmit is still mapped to one out of M possible pulse off-on edge start offsets. However, the duty cycle of each pulse can be varied to control the average amount of flux emitted and thus illumination levels. Reference (Rajagopal et al., 2012) outlines using VPPM for illumination and communication.

1.3.4 Optical orthogonal frequency division multiplexing

OFDM is a spectrally efficient modulation technique and has been widely adopted for RF wireless communications. In OFDM, parallel streams of information are mapped over orthogonal frequency bins. Each bin is called a sub-carrier. Usually an M-ary QAM modulation is used to map information over each sub-carrier. An IFFT operation multiplexes the parallel streams to generate a time domain OFDM symbol to transmit. To mitigate interference due to multi-path, usually a CP is appended to the symbol before transmitting it. At the receiver, after removing the CP, an FFT operation demultiplexes the OFDM symbol to recover the parallel sub–carriers. Each sub-carrier is then demodulated to recover the information. OFDM has been successfully adapted and widely used for spectrally efficient OWC as summarized in reference (Armstrong, 2009). For OWC, the time domain OFDM symbol is constrained to be real valued and unipolar. Ensuring Hermetian symmetry during symbol mapping over the orthogonal frequency bins will generate a real valued time domain signal. Figure 2·5 illustrates signaling chain for O-OFDM.

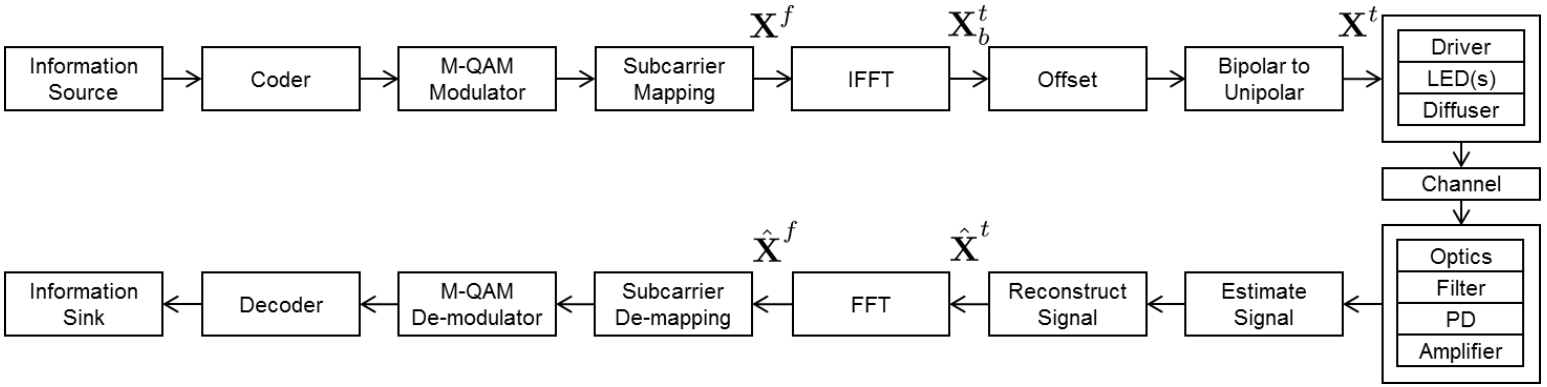

Figure 1·5: Optical OFDM block diagram

Let N_{sc} be the total number of sub-carriers for the O-OFDM frame. In DCO-OFDM, the information bits are mapped to $N_{dco}^{d} = (N_{sc}/2) - 1$ number of data sub-carriers. An M-QAM modulator then assigns an M-QAM symbol corresponding the mapped bits on the data sub-carriers. The remaining sub-carriers are assigned Hermetian symmetric M-QAM symbols to form the frequency domain DCO-OFDM frame as shown in Eq.(2.12).

$$\mathbf{X}^{f} = [0; x_1; \ldots; x_{N_{dco}^{d}}; 0; x_{N_{dco}^{d}}^{*}; \ldots; x_1^{*}] \tag{1.12}$$

Taking an IFFT over frame $\mathbf{X}^{f}$ generates a bipolar time domain symbol $\mathbf{X}_b^{t}$. In DCO-OFDM the bipolar to unipolar conversion involves adding an offset to $\mathbf{X}_b^{t}$ such that majority of the the time domain symbol is non-negative and the symbol can then be clipped at zero. For relatively large N_{sc}, the signal values in the time domain are distributed normally. Thus adding an offset of at least 3.2×SD ensures that less than 0.1% of signal values get clipped at zero - thus significantly reducing signal distortion due to clipping at the transmitter.

In ACO-OFDM, only the odd indexed sub-carriers carry data symbols. Hermetian symmetry is then enforced to obtain real valued time domain symbol. The information bits are mapped to $N_{aco}^{d} = (N_{sc}/4)$ number of data sub-carriers. An M-QAM modulator then assigns an M-QAM symbol corresponding the mapped bits on the data sub-carriers. The frequency domain ACO-OFDM frame construction is shown in Eq.(2.13).

$$\mathbf{X}^{f} = [0; x_1; 0; x_2; \ldots; x_{N_{aco}^{d}}; 0; x_{N_{aco}^{d}}^{*}; \ldots; 0; x_2^{*}; 0; x_1^{*}] \tag{1.13}$$

Taking an IFFT over frame $\mathbf{X}^{f}$ generates a bipolar time domain symbol $\mathbf{X}_b^{t}$. In ACO-OFDM bipolar to unipolar conversion is achieved by simply clipping the symbol at zero. It has been shown in reference (Armstrong and Lowery, 2006) that this clip-

ping introduces noise only on the non-data bearing even indexed sub-carriers. Thus by simple signal processing, an estimate of transmitted signal can be reconstructed. The N_{aco}^{d} data sub-carriers are then demodulated and decoded to recover transmitted information. Implementation and performance comparisons of ACO-OFDM and DCO-OFDM is shown in reference (Mesleh et al., 2011).

References

Armstrong, J. (2009). Ofdm for optical communications. *Lightwave Technology, Journal of*, 27(3):189 –204.

Armstrong, J. and Lowery, A. (2006). Power efficient optical ofdm. *Electronics Letters*, 42(6):370 – 372.

Bai, B., Xu, Z., and Fan, Y. (2010). Joint led dimming and high capacity visible light communication by overlapping ppm. In *Wireless and Optical Communications Conference (WOCC), 2010 19th Annual*, pages 1–5.

Barry, J. R. (1994). *Wireless Infrared Communications*. Kluwer Academic Publishers, Norwell, MA, USA.

Grubor, J., Randel, S., Langer, K.-D., and Walewski, J. (2008). Broadband information broadcasting using led-based interior lighting. *Lightwave Technology, Journal of*, 26(24):3883–3892.

Kahn, J. and Barry, J. (1997). Wireless infrared communications. *Proceedings of the IEEE*, 85(2):265 –298.

Komine, T. and Nakagawa, M. (2004). Fundamental analysis for visible-light communication system using LED lights. *Consumer Electronics, IEEE Transactions on*, 50(1):100 – 107.

Mesleh, R., Elgala, H., and Haas, H. (2011). On the performance of different ofdm based optical wireless communication systems. *Optical Communications and Networking, IEEE/OSA Journal of*, 3(8):620 –628.

Rajagopal, S., Roberts, R., and Lim, S.-K. (2012). IEEE 802.15.7 visible light communication: modulation schemes and dimming support. *Communications Magazine, IEEE*, 50(3):72–82.

Vucic, J., Kottke, C., Nerreter, S., Habel, K., Buttner, A., Langer, K.-D., and Walewski, J. (2009). 125 mbit/s over 5 m wireless distance by use of ook-modulated phosphorescent white leds. In *Optical Communication, 2009. ECOC '09. 35th European Conference on*, pages 1 –2.